

## Supporting Information: Velocity Profile Shape Factors for Core-Annular Flow (CAF)

One dimensional Two-Fluid models which are used to model transient and undeveloped annular flows require introducing correction factors on the inertia terms, which are expressed in terms of the average phase velocity. These are denoted as the velocity profile 'shape factors', and their definition evolve from the averaging of the phase's inertia over the flow cross section. Accordingly, the shape factors are defined by:

The above area-averaged shape-factor for the annular phase is obtained by:

$$\gamma_a = \frac{\int_{A_a} u_a^2 dA_a}{A_a U_a^2} = \frac{\varepsilon_a}{\pi q^2} \int_{\xi_w}^{\xi_c} d\xi \int_0^{2\pi} \tilde{u}_a^2 J d\phi \quad (S1.1)$$

$$\gamma_c = \frac{\int_{A_c} u_c^2 dA_c}{A_c U_c^2} = \frac{(1-\varepsilon_a)}{\pi} \int_{\xi_c}^{\infty} d\xi \int_0^{2\pi} \tilde{u}_c^2 J d\phi \quad (S1.2)$$

### Horizontal flows:

In 1D (Two-Fluid, TF) models the flows of the annular and core phases are represented in terms of the holdup and average velocity. The velocity profile shape factors represent the corrections to be introduced on the inertia terms the TF model is used to simulate transient or undeveloped CAFs. As the velocity profiles are not resolved in the framework of 1-D Two-Fluid models, plug flow is usually assumed in both phases. The velocity profiles obtained by the exact solutions can be used to test the validity of the plug flow assumption and to calculate the velocity profile shape factors that should be introduced in the Two-Fluid models in order to correctly represent the phases' inertia.

The effects of the core eccentricity and viscosity ratio on the velocity profile shape factors of the core and annular phases in horizontal CAF ( $Y=0$ ) are demonstrated in Figures (S1) and (S2). In horizontal flow the velocity profiles and the shape factors are not affected by the phases' density ratio, and the reference to the density of the phases is maintained in the notation only for the sake of consistency with previous results.

Figures (S1a,b) are for the case of  $\mu_a/\mu_c = \mu_H/\mu_L = 0.1$ , where the less viscous (heavy) phase flows in the annulus, while the viscous (light) phase flows in the core. As seen in Figure (S1a), in the limit of concentric CAF, the shape factor value of the annular phase is  $\gamma_a = 4/3$  independently of the holdup and of the viscosity ratio. See Eq. (35.1) and Figure (S2a). Obviously, also in the limit of  $\varepsilon_a \rightarrow 1$ , the value of  $\gamma_a \rightarrow 4/3$  (which corresponds to single-phase Pouisille flow) is reached independently of the core eccentricity and viscosity. However, in the limit of  $\varepsilon_a \rightarrow 0$ , as well as for moderate holdups of the annular phase, the value of the shape factor is sensitive to the core eccentricity, in particular in the range of low core eccentricities. Figure (S2a) shows that the sensitivity of  $\gamma_a$  to deviations from concentric CAF configurations (nonzero E) becomes even more pronounced for  $\tilde{\mu} \geq 1$  (the annular phase is more viscous), and persist over a wider range of holdups. For high core eccentricities, say  $E > 0.7$ , the shape factor values become similar to those obtained with fully eccentric CAF model.

Figure (S1b) shows the shape of the phase factor in the core,  $\gamma_c$  for the case of  $\tilde{\mu} = 0.1$ . As expected, for low holdups of the annular phase,  $\gamma_c$  is insensitive to the core eccentricity and its variations with the holdup and with the viscosity ratio (see Figure (S2b)) follow those obtained with concentric CAF (see Eq. (35.2)). The insensitivity of  $\gamma_c$  to the core eccentricity extends over a wider range of holdups for  $\tilde{\mu} \geq 1$ . In the other limit of  $\varepsilon_a \rightarrow 1$  (i.e., the core phase vanishes) and  $\gamma_c \rightarrow 1$  independently of the core eccentricity and viscosity ratio. As implied by Figure (S2b), for  $\tilde{\mu} \gg 1$ , i.e.,  $\tilde{\mu} \rightarrow \infty$ ,  $\gamma_c \rightarrow 4/3$  practically for the whole range of holdups (except when the core vanishes, where  $\gamma_c \rightarrow 1$ ). This is obviously expected, since the case of  $\tilde{\mu} \rightarrow \infty$  corresponds to single phase Poiseuille flow of the core phase through a (concentric or eccentric) cavity.

### Inclined flows:

While in horizontal flow the shape factor are practically bounded,  $1 \leq \gamma_c, \gamma_a \approx 1.5$ , this is not the case in inclined flows, where the shape factors can attain very large values. The large values correspond to conditions of backflow, where part of the fluid is flowing opposite to the superficial velocity direction. Hence, backflow refers to downward flow in the heavy phase near the wall in concurrent up-flow, or upward flow of the heavy phase near the interface in countercurrent flow. Similarly, backflow of the light phase refers to its upward flow near the upper wall in concurrent downward flow, or down flow of the light phase near the interface in countercurrent flow.

The effect of the core eccentricity on the shape factors of the phases in inclined CAF is demonstrated in Figure S3. This figure corresponds to the case where the annular phase is heavier and less viscous,  $\mu_a/\mu_c = \mu_H/\mu_L = 0.1$ . The constant inclination parameter ( $Y = -5$ ) is scaled with the superficial frictional pressure gradient of the light (core) phase. As shown in Figure (S3a), the gravity has a pronounced effect on the shape factor of the heavier phase. The escalation of the heavy phase shape factors takes place both in concurrent and countercurrent flows while approaching  $X^2 = 0$  (with non-zero holdup), where the velocity profile corresponds to recirculating flow. At  $X^2 = 0$  the nonzero middle and highest holdup solutions (see Figure 5 in the paper),  $\gamma_a \rightarrow \infty$ . The general trends of the variation of the shape factors of the heavy and light phase are exhibited by the case of concentric CAF ( $E = 0$ ), that can be easily calculated by applying the analytical expressions (Eqs. 36-37). However, the effect of the core eccentricity on the shape factor of the heavy (annular) phase (Figure S3a) can be pronounced, in particular for  $E > 0.3$ , and is non-monotonous in the countercurrent region. As expected, the shape factor of the core (light) phase is less sensitive to the core eccentricity (Figure S3b). The core eccentricity effect becomes pronounced at steeper inclinations, in particular in the countercurrent flow region (Figure S3c).

Increasing the viscosity of the heavy phase reduces the effect of gravity suppresses the backflow in the heavy phase (near the wall) in concurrent up-flow and reduces the countercurrents flow region. Consequently, as shown in the Figure (S4a) the shape factors of the heavy phase are reduced and become similar to those obtained in horizontal flow. Also, the effect of the eccentricity becomes less pronounced with increasing the annular (heavy) phase viscosity. Figure (S4b) shows that in the concurrent up-flow region, the values of the shape factors of the core (light) phase ranges between 1 to 4/3, similarly to the values obtained in horizontal

CAF, and the values increase with reducing the core viscosity (increasing  $\tilde{\mu}$ ). Yet, as shown in Figure (S3c), much higher values are obtained for  $\gamma_L$  at steeper inclinations, however only in the countercurrent region, where also the effect of core eccentricity becomes more pronounced.

Figure (S5a,b) show the effect of the core eccentricity on the shape factors in case the less viscous heavy phase flows in the core. In fact, this is the reversed case of Figure (S3). Here too, the  $Y=-5$  is scaled with the superficial frictional pressure gradient of the light (annular) phase. In general, the trends of the heavy phase shape factors appear similar to those shown in Figure (S3). However, the countercurrent region is shifted to lower holdups, and the effect of the core eccentricity on the shape factor values is monotonic: The shape factor of the heavy core phase increases with reducing the core eccentricity, whereby the core phase is less affected by the presence of the wall. It is interesting to note that in the concurrent up-flow region; values of the shape factor very close to 1 are obtained, indicating that the velocity profile is almost flat, due to the opposite effects of the shear and gravity on the velocity profile of the core phase. The effect of the core eccentricity on the shape factor of the annular phase is monotonous, whereby increasing values obtained at higher eccentricities (with the exception of  $E \rightarrow 1$  where the less viscous core touches the wall).

In experimental studies only the velocity profile along the pipe centerline is measured and is often used to deduce the velocity profile shape factor. The center-line shape factors when defined with respect to the inertia of the area-averaged velocity are given by:

$$\gamma_{as}^0 = \frac{\varepsilon_a^2}{2(1-\tilde{R}_c)q^2} \int_{\xi_w}^{\xi_c} \left( \tilde{u}_a^2|_{\phi=0} + \tilde{u}_a^2|_{\phi=\pi} \right) H_\phi d\xi \quad (\text{S2.1})$$

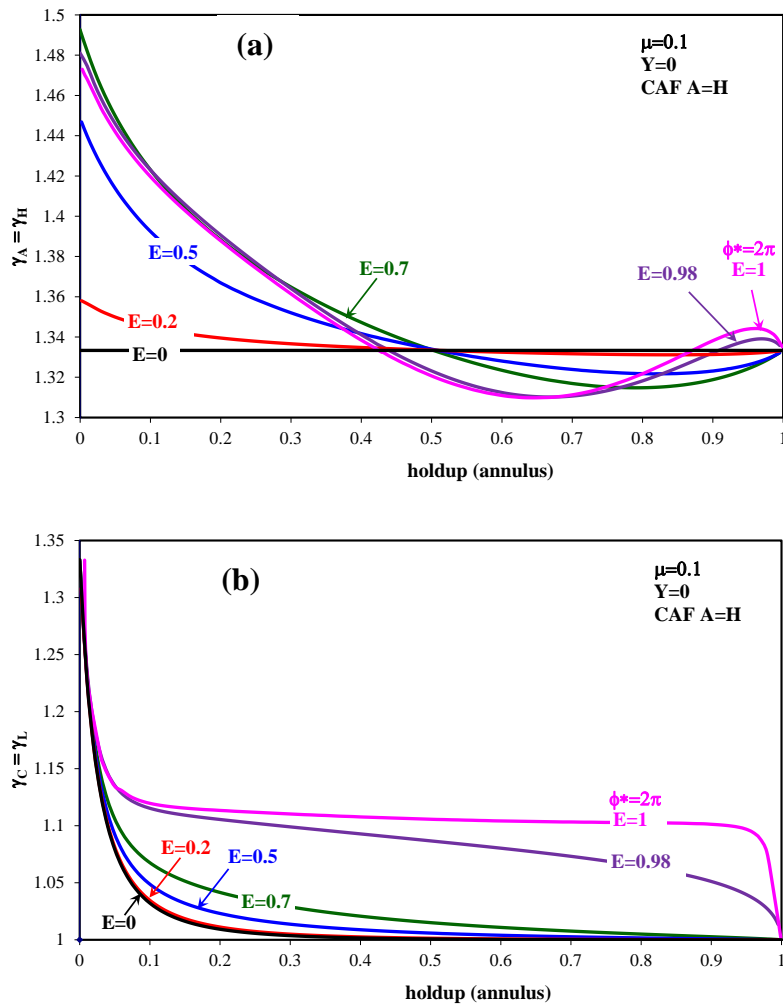
$$\gamma_{cs}^0 = \frac{(1-\varepsilon_a)^2}{2\tilde{R}_c} \int_{\xi_c}^{\infty} \left( \tilde{u}_c^2|_{\phi=0} + \tilde{u}_c^2|_{\phi=\pi} \right) H_\phi d\xi \quad (\text{S2.2})$$

The center-line shape factors, when defined with respect to the inertia of the center-line average velocity, are obtained by:

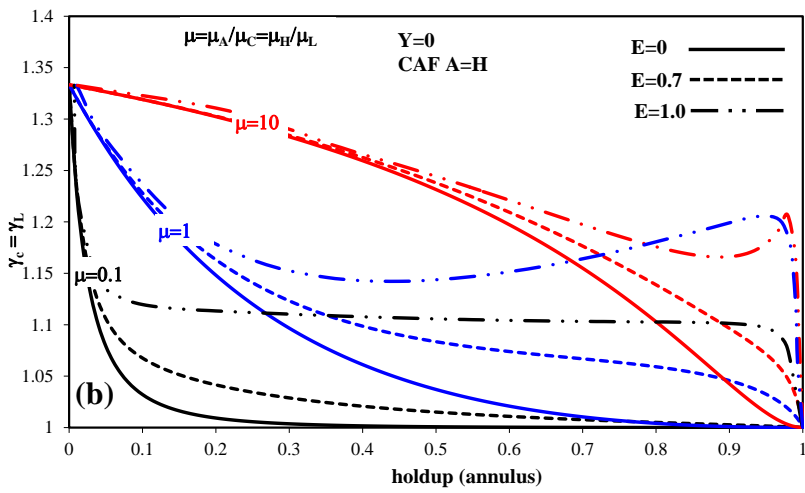
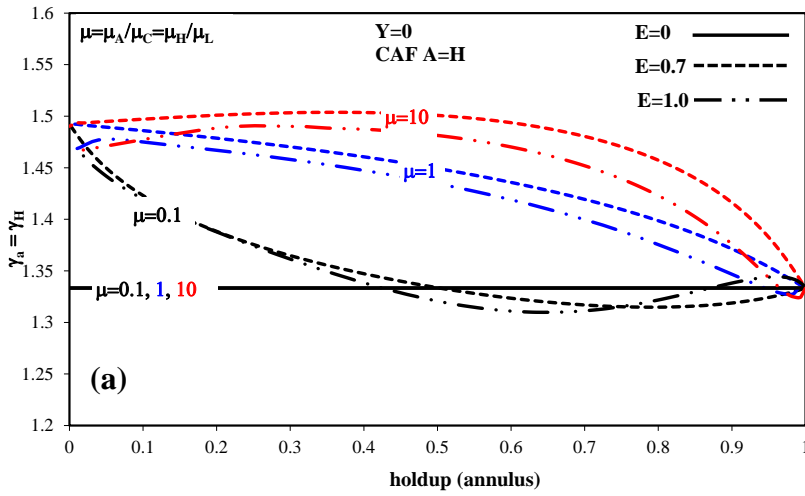
$$\gamma_a^0 = 2(1-\tilde{R}_c) \frac{\int_{\xi_w}^{\xi_c} \left( \tilde{u}_a^2|_{\phi=0} + \tilde{u}_a^2|_{\phi=\pi} \right) H_\phi d\xi}{\left( \int_{\xi_w}^{\xi_c} \left( \tilde{u}_a|_{\phi=0} + \tilde{u}_a|_{\phi=\pi} \right) H_\phi d\xi \right)^2} \quad (\text{S3.1})$$

$$\gamma_c^0 = 2\tilde{R}_c \frac{\int_{\xi_c}^{\infty} \left( \tilde{u}_c^2|_{\phi=0} + \tilde{u}_c^2|_{\phi=\pi} \right) H_\phi d\xi}{\left( \int_{\xi_w}^{\xi_c} \left( \tilde{u}_c|_{\phi=0} + \tilde{u}_c|_{\phi=\pi} \right) H_\phi d\xi \right)^2} \quad (\text{S3.2})$$

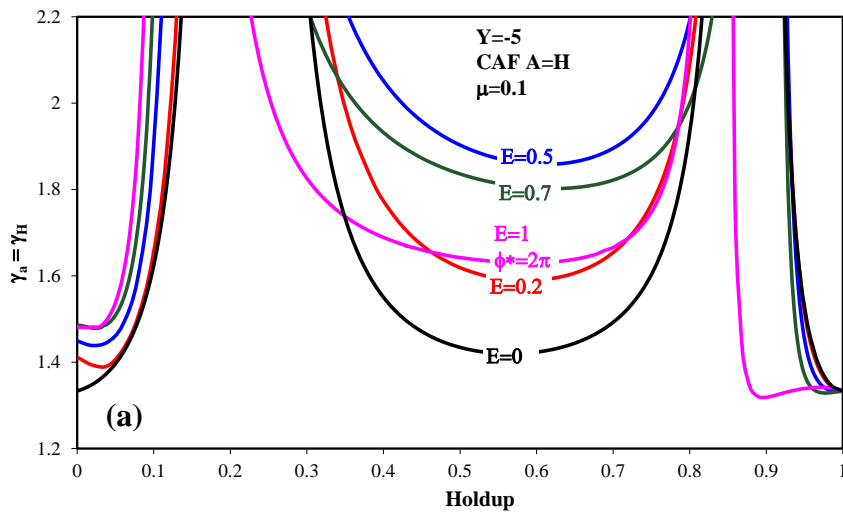
In the limit of  $E \rightarrow 0$ , using the closed-form analytical solution for the velocity profiles of the core and annular phases (Eqs. 18) in Eqs.(34) yields a closed form expressions for the shape factors of the core and annular phases:



**Fig. S1:** Effect of the annular (heavy) phase holdup and core eccentricity on the velocity-profile shape factors for the case of horizontal CAF flow with  $\tilde{\mu} = 0.1$ . The less viscous (heavy) phase flows in the annulus **(a)** Shape factor of the annular phase, **(b)** shape factor of the core (viscous, light) phase.



**Fig. S2:** Effect of the annular (heavy) phase holdup, core eccentricity and viscosity ratio on the velocity-profile shape factors for the case of horizontal CAF flow with various viscosity ratios. (a) shape factor of the annular (heavy) phase (b) shape factor of the core (light) phase.



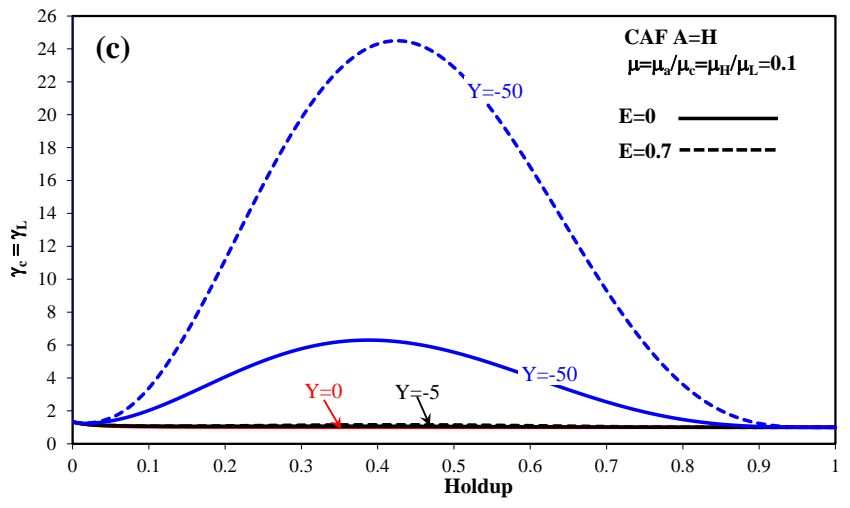
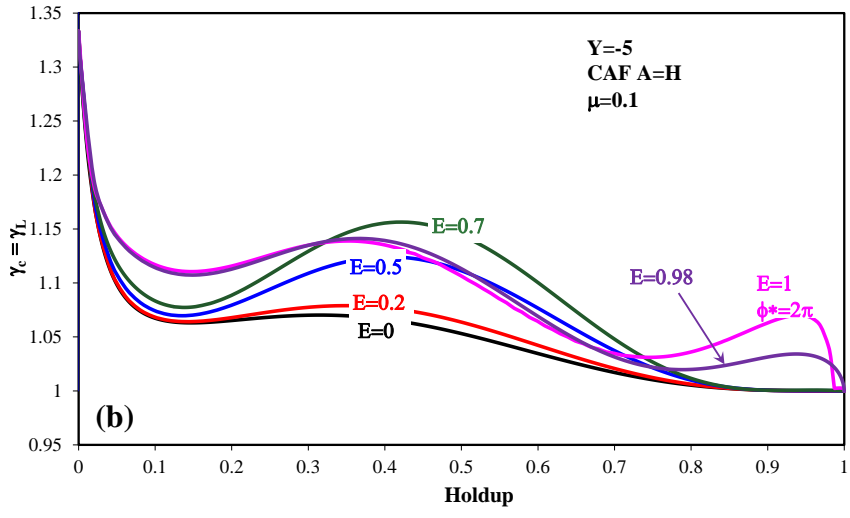


**Fig. S3:** The effect of the holdup and core eccentricity on the shape factors in case the annular phase is heavier and less viscous. (a) annular phase,  $Y=-5$  (b) core phase,  $Y=-5$ . (c) core phase- effect of  $Y$ .

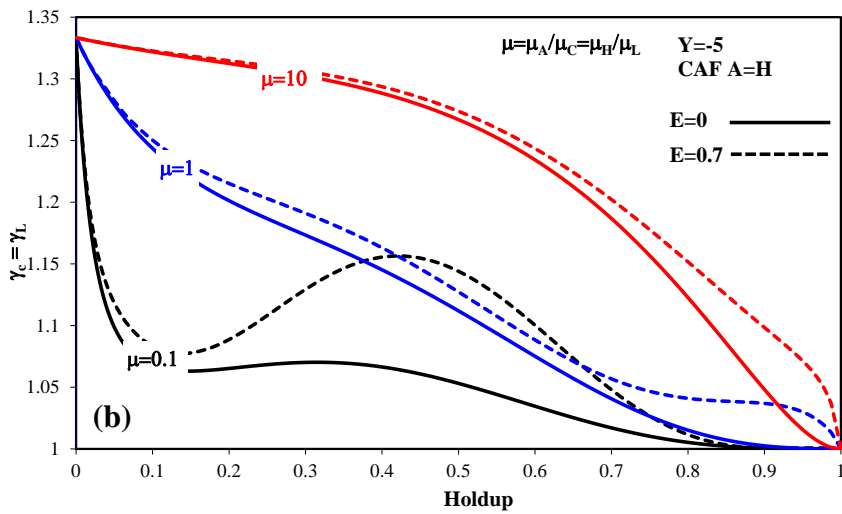
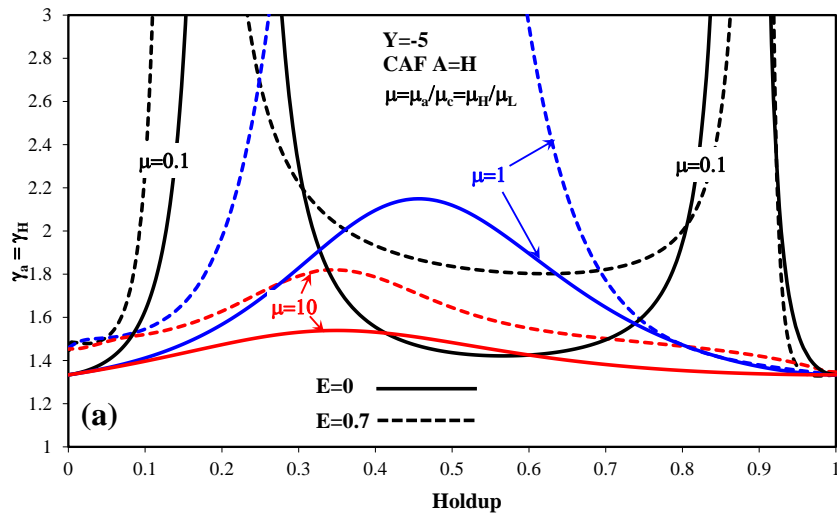


**Fig. S4:** The effect of the holdup and viscosisty ratio on the shape facotrs of the annular (a) and core (b) phases, in inclined flow,  $Y=-5$ , where the annular phase is heavier.

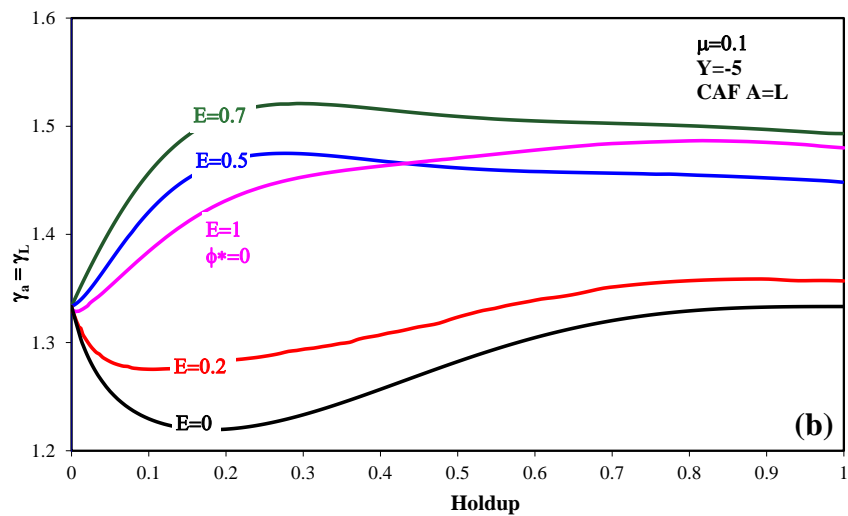
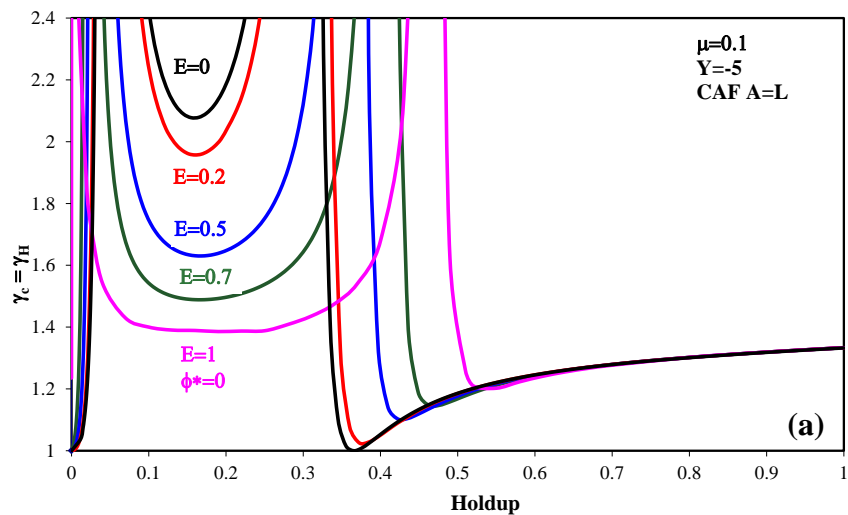


**Fig. S5:** The effect of the holdup and core eccentricity on the shape factors of the core (a) and annular (b) phases, in case the annular phase is lighter and less viscous.



## Supporting Information: Cartesian and Bipolar Coordinates for Core-Annular Flow

Referring to Figure 1, where the origin  $(x,y=0,0)$  is set in the pipe center and considering a transformation  $\tilde{z}$ -plane  $\tilde{z} = \tilde{x} + i\tilde{y}$  to a  $\omega$ -plane,  $\omega = \xi + i\phi$ , where  $\tilde{x}, \tilde{y}, \tilde{z}$  denote dimensionless scale (normalized by  $R$ ):

$$\omega = \ln \left( \frac{\tilde{z} - ie^{\xi_w}}{\tilde{z} - ie^{-\xi_w}} \right) \quad (\text{A.1})$$

Whereby:

$$\tilde{z} = \frac{i(e^{-\xi_w}e^\omega - e^{\xi_w})}{e^\omega - 1} = \frac{-i \cosh \xi_w \cos \phi + i \cosh(\xi - \xi_w) - \sinh \xi_w \sin \phi}{\cosh \xi - \cos \phi} \quad (\text{A.2})$$

Accordingly,  $x = x(\xi, \phi)$ ;  $y = y(\xi, \phi)$  are given by:

$$\tilde{x} = -\frac{\sinh \xi_w \sin \phi}{\cosh \xi - \cos \phi} \quad ; \quad \tilde{y} = \frac{\cosh(\xi - \xi_w) - \cosh \xi_w \cos \phi}{\cosh \xi - \cos \phi} \quad (\text{A.3})$$

The polar coordinate,  $\tilde{r} = r/R$  is therefore given by:

$$\tilde{r}^2 = 1 - \frac{2 \sinh \xi_w \sinh(\xi - \xi_w)}{\cosh \xi - \cos \phi} \quad (\text{A.4})$$

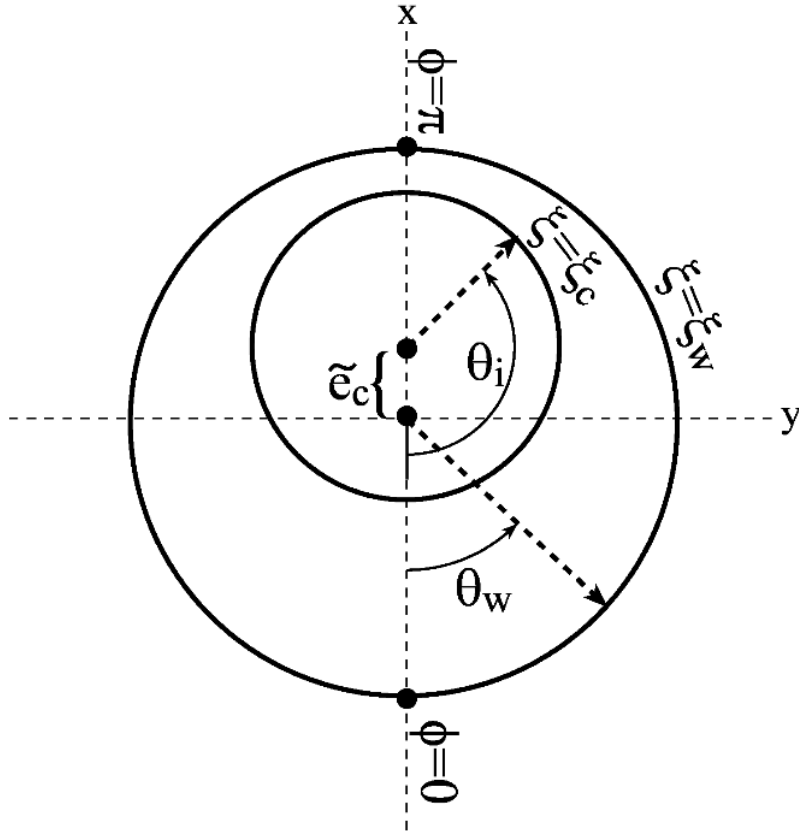


**Figure A.1:** Geometrical variables used to define distances along the interface and the wall in the CAF model.

Using Eq. (A.3), a point on the interface corresponds to  $\xi = \xi_c$  (see Figure A.1) where:

$$\tilde{y}^* = \frac{\cosh(\xi_c - \xi_w) - \cosh \xi_w \cos \phi}{\cosh \xi_c - \cos \phi}; \quad (\text{A.5})$$

The  $\xi_c(\tilde{e}_c, \tilde{R}_c)$ ,  $\xi_w(\tilde{e}_c, \tilde{R}_c)$  are determined Eq. (4) and  $\tilde{e}_c = E(1 - \tilde{R}_c)$ . Accordingly, a point on the core interface corresponds to:

$$\theta_i = \cos^{-1} \frac{e - \tilde{y}^*}{\tilde{R}_c} = \cos^{-1} \frac{1}{\tilde{R}_c} \left[ E(1 - \tilde{R}_c) - \frac{\cosh(\xi_c - \xi_w) - \cosh \xi_w \cos \phi}{\cosh \xi_c - \cos \phi} \right] \quad (\text{A.6})$$

The distance along the core interface (measured from the point on the pipe meridian which is the farer from the pipe wall) is then given by:

$$\frac{1}{2} \tilde{s}_i = \tilde{R}_c \cos^{-1} \frac{e - \tilde{y}^*}{\tilde{R}_c} = \tilde{R}_c \cos^{-1} \frac{1}{\tilde{R}_c} \left[ E(1 - \tilde{R}_c) - \frac{\cosh(\xi_c - \xi_w) - \cosh \xi_w \cos \phi}{\cosh \xi_c - \cos \phi} \right]; 0 \leq \phi \leq \pi \quad (\text{A.7})$$

For  $\phi = \pi$ , Eq. (A.7) yields the expected result,  $\tilde{s}_i / 2 = \pi \tilde{R}_c$ .

The distance along the pipe wall (measured from the point on the pipe meridian which is the farer from the core interface) is then given by:

$$\theta_w = \frac{1}{2} \tilde{s}_w = \pi - \cos^{-1} \tilde{y}_w = \pi - \cos^{-1} \frac{1 - \cosh \xi_w \cos \phi}{\cosh \xi_w - \cos \phi}; 0 \leq \phi \leq \pi \quad (\text{A.8})$$

As expected, for  $\phi = \pi$ , Eq. (A.8) yields  $\tilde{s}_w / 2 = \pi$ .

**For fully eccentric core**, the uni-polar coordinate has been used, where:

$$\tilde{y} = \frac{2\xi_1}{\xi_1^2 + \xi_2^2}; \quad \tilde{x} = \frac{2\xi_2}{\xi_1^2 + \xi_2^2}; \quad (\text{A.9})$$

A point on the core interface corresponds to  $\xi_1 = \xi_c = 1/\tilde{R}_c$ , where its y coordinate is :

$$\tilde{y}^* = \frac{2\xi_c}{\xi_c^2 + \xi_2^2} \quad (\text{A.10})$$

Accordingly, a point on the core interface corresponds to (see Figure (A.2)) :

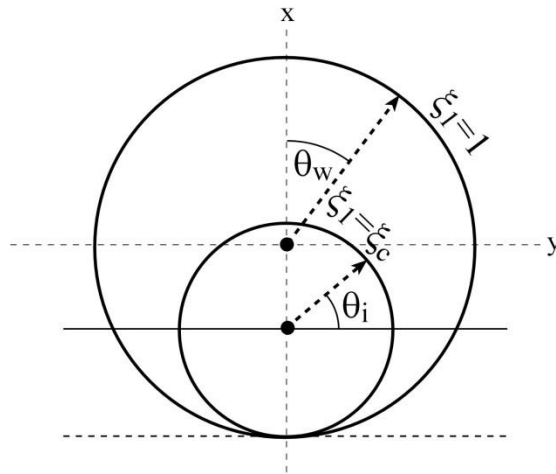


**Figure A.6:** Geometrical variables used to define distances along the interface and the wall in the FE CAF model.

$$\theta_i = \cos^{-1} \frac{\tilde{y}^* - \frac{1}{\xi_c}}{\tilde{R}_c} = \cos^{-1} \left[ \frac{\xi_c^2 - \xi_2^2}{\xi_c^2 + \xi_2^2} \right] \quad (\text{A.11})$$

The distance along the core interface (measured from the point on the pipe meridian which is the farer from the pipe wall) is then given by: (A.10)

$$\frac{1}{2} \tilde{s}_i = \frac{1}{\xi_c} \cos^{-1} \left[ \frac{\xi_c^2 - \xi_2^2}{\xi_c^2 + \xi_2^2} \right]; \quad 0 \leq \xi_2 \leq \infty \quad (\text{A.12})$$

At the TP, where  $\xi_2 \rightarrow \infty$ ,  $\tilde{s}_i / 2 = \pi \tilde{R}_c$ , and  $\tilde{y}_w = 2 / (1 + \xi_2^2)$ .

The distance along the pipe wall (measured from the point on the pipe meridian which is the farer from the core interface) is then given by  $\theta_w$ :

$$\theta_w = \frac{1}{2} \tilde{s}_w = \cos^{-1} (\tilde{y}_w - 1) = \cos^{-1} \left[ \frac{2}{1 + \xi_2^2} - 1 \right] = \cos^{-1} \left[ \frac{1 - \xi_2^2}{1 + \xi_2^2} \right]; \quad 0 \leq \xi_2 \leq \infty \quad (\text{A.13})$$

As expected, at the TP, where  $\xi_2 \rightarrow \infty$ ,  $\tilde{s}_w / 2 = \pi$ .